20th International Conference on Structural Mechanics in Reactor Technology (SMiRT 20)
Espoo, Finland, August 9-14, 2009
SMiRT 20-Division 3, Paper 2045

An Implicit Solution Framework for Reactor Fuel Performance Simulation

Glen Hansen, Chris Newman, Derek Gaston, and Cody Permann

Multiphysics Methods Group, Idaho National Laboratory, Idaho Falls, Idaho, USA
e-mail: glen.hansen@inl.gov

Keywords: reactor multiphysics, nuclear fuel performance, fuel thermomechanics.

1 ABSTRACT

The simulation of nuclear reactor fuel performance involves complex thermomechanical processes between fuel pellets, made of fissile material, and the protective cladding that surrounds the pellets. An important design goal for a fuel is to maximize the life of the cladding thereby allowing the fuel to remain in the reactor for a longer period of time to achieve higher degrees of burnup. This paper presents an initial approach for modeling the thermomechanical response of reactor fuel, and details of the solution method employed within INL's fuel performance code, BISON.

The code employs advanced methods for solving coupled partial differential equation systems that describe multidimensional fuel thermomechanics, heat generation, and oxygen transport within the fuel. This discussion explores the effectiveness of a JFNK-based solution of a problem involving three dimensional fully coupled nonlinear transient heat conduction and that includes pellet displacement and oxygen diffusion effects. These equations are closed using empirical data that is a function of temperature, density, and oxygen hyperstoichiometry. The method appears quite effective for the fuel pellet / cladding configurations examined, with excellent nonlinear convergence properties exhibited on the combined system. In closing, fully coupled solutions of three dimensional thermomechanics coupled with oxygen diffusion appear quite attractive using the JFNK approach described here, at least for configurations similar to those examined in this report.

2 INTRODUCTION

BISON is built upon a code framework based on tight coupling of two and three dimensional fuel physics models that employ physics-based preconditioned Jacobian-free Newton-Krylov solution methods using modern software engineering principles. Goals of the code are to perform higher fidelity calculation of two and three dimensional pellet cladding mechanical interaction and to support advanced models to provide a parallel analysis and design capability.

Significant progress has been achieved toward developing a fully-coupled solution methodology for thermomechanics coupled to oxygen diffusion and in creating a base multidimensional thermomechanics code that employs these solution methods on UO_2 fuel pellet geometries. BISON is being developed using modern software engineering principles resulting in a code that is inexpensive to maintain as well as meeting software quality goals. This study illustrates the efficacy of this approach for three-dimensional parallel thermomechanics coupled with oxygen diffusion run on up to 1024 processors.

3 THEORETICAL BACKGROUND

The results presented in this paper are based on a solution of three fully coupled partial differential equations for heat conduction, oxygen diffusion, and linear elastic solid mechanics. Let Ω define the fuel pellet domain. The heat conduction model assumes fission reactions generate heat at a uniformly distributed constant rate Q,

$$
\begin{aligned}
\rho C_p T_t - \nabla \cdot k \nabla T - Q = &\ 0 \qquad && T \in \Omega, \\
T = &\ T_d \qquad && T \in \Gamma^D, \\
n \cdot \nabla T = &\ 0 \qquad && T \in \Gamma^N, \\
T(t=0) = &\ T_0 \qquad && T \in \Omega,
\end{aligned}
$$

where *T*, ρ, *Cp* and *k* are temperature, density, specific heat and thermal conductivity. Here, Γ^N denotes the top and bottom boundary of the fuel pellet and Γ^D denotes the outer circumferential fuel pellet boundary. The model for oxygen diffusion *s* is given by

$$
\begin{aligned}
s_t - \nabla \cdot (D(\nabla s + \frac{sQ^*}{FRT^2} \nabla T)) = &\ 0 \qquad && s \in \Omega, \\
s = &\ s_d \qquad && s \in \Gamma^D, \\
s(t=0) = &\ s_0 \qquad && s \in \Omega,
\end{aligned}
$$

where *D* is the diffusivity of UO_2, *F* is the thermodynamic factor of oxygen, *Q** is the heat of transport of oxygen and *R* is the universal gas constant. The solid mechanics model for the displacement **u** is given by

$$
\begin{aligned}
\mathbf{u}_{tt} - \mathrm{A}^{\mathrm{T}} \mathrm{D} \mathrm{A} \mathbf{u} + f = &\ 0 \qquad && \mathbf{u} \in \Omega, \\
\mathbf{u} = &\ 0 \qquad && \mathbf{u} \in \gamma^D, \\
\mathbf{u}(t=0) = &\ \mathbf{u}_0 \qquad && \mathbf{u} \in \Omega, \\
\mathbf{u}_t(t=0) = &\ \mathbf{u}_{00} \qquad && \mathbf{u} \in \Omega,
\end{aligned}
$$

with

$$
\mathrm{A} = \begin{bmatrix} \partial_x & 0 & 0 \\ 0 & \partial_y & 0 \\ 0 & 0 & \partial_z \\ \partial_y & \partial_x & 0 \\ 0 & \partial_z & \partial_y \\ \partial_z & 0 & \partial_x \end{bmatrix}, \quad \mathrm{D} = c_1 \begin{bmatrix} 1 & c_2 & c_2 & 0 & 0 & 0 \\ c_2 & 1 & c_2 & 0 & 0 & 0 \\ c_2 & c_2 & 1 & 0 & 0 & 0 \\ 0 & 0 & 0 & c_3 & 0 & 0 \\ 0 & 0 & 0 & 0 & c_3 & 0 \\ 0 & 0 & 0 & 0 & 0 & c_3 \end{bmatrix}
$$

and

$$
c_1 = \frac{E(1-\nu)}{(1+\nu)(1-\nu)}, \quad c_2 = \frac{\nu}{(1-\nu)}, \quad c_3 = \frac{(1-2\nu)}{2(1-\nu)}.
$$

The coefficients *E* and ν are Young's modulus and Poisson's ratio. The forcing term *f* weakly enforces thermal expansion, and γ^D denotes the pellet bottom. The quantities *Q*, ρ, *Cp*, *k*, *D*, *Q**, *F* and *E* in the above and the constitutive models in f are given by nonlinear empirical functions of *T*, *s* and **u**. These constitutive and closure relations are from Ramirez et. al. (2006) and Hohorst (1990) (see Newman et. al. 2009 for specific details).

This system of equations is discretized using a standard finite element method, using the approach advanced by Newman et. al. (2009). In this approach, the resulting nonlinear algebraic system is expressed in the form

$$
\mathrm{F}(\mathrm{x}) = 0 \,,
$$

that is of length *N* unknowns. This system is then solved using a Jacobian-free Newton Krylov method (see Knoll and Keyes (2004) and references contained therein). If one applies Newton's method to the above, a linear system results

$$
\mathcal{J}(\mathrm{x}^{(k)}) \, \delta \mathrm{x}^{(k)} = -\mathrm{F}(\mathrm{x}^{(k)}),
$$

where *J* is the Jacobian of the system and *k* is the iteration counter for the Newton iteration. It is usually necessary to solve the preconditioned form of this system in engineering applications,

$$
\mathcal{J}(\mathrm{x}^{(k)}) \, M^{-1} (M \delta \mathrm{x}^{(k)}) = -\mathrm{F}(\mathrm{x}^{(k)}),
$$

where M^{-1} represents the preconditioning process. The iteration is advanced to the next step using

$$\mathrm{x}^{(k+1)} \longleftarrow \mathrm{x}^{(k)} + \delta\mathrm{x}^{(k)}.$$

When a Krylov method such as GMRES (Saad (1995)) is used to solve the linear system, it is not necessary to compute or store the Jacobian of the system, as only the action of the Jacobian on a vector is needed to solve the linear problem. The action may be approximated using a finite difference approximation,

$$\mathcal{J}(\mathrm{x}^{(k)})M^{-1}\mathrm{v} \approx \frac{\mathbf{F}(\mathrm{x}^{(k)} + \varepsilon M^{-1}\mathrm{v}) - \mathbf{F}(\mathrm{x}^{(k)})}{\varepsilon}$$

and hence this solution method is named a Jacobian-free Newton Krylov (JFNK) method. Effective preconditioning must typically be used for efficiency. These results employ a physics-based preconditioner based a lower triangular approximate system

$$\mathbf{M} = \begin{bmatrix} (R_1)_T & 0 \\ (R_2)_T & (R_2)_s \end{bmatrix}$$

by solving

$$(R_1)_g \mathbf{q}_1 = v_1,$$
$$(R_2)_h \mathbf{q}_2 = v_2 - (R_2)_g \mathbf{q}_1,$$

where **q** represents the action of M^{-1} on *v* (e.g. approximately solving M**q** = *v*). Alternatively, one may employ a diagonal decoupled preconditioner

$$\begin{bmatrix} (R_1)_T & 0 \\ 0 & (R_2)_s \end{bmatrix}$$

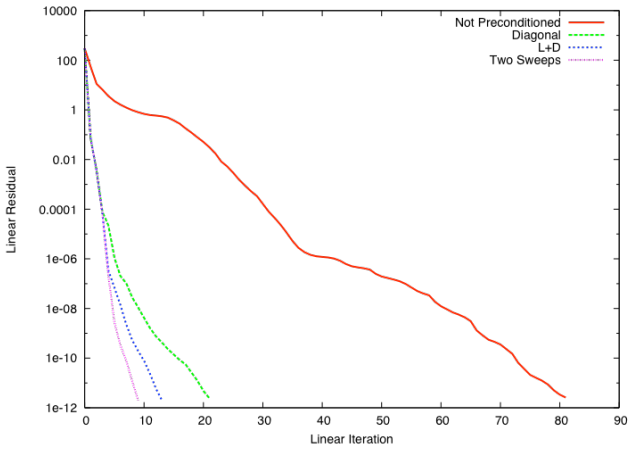

Figure 1. Number of linear iterations (effort) needed to achieve a given level of accuracy using various preconditioning choices on a coupled thermomechanics problem.

Figure 1 shows a representative calculation on a thermomechanics problem of the performance of various preconditioners applied in a JFNK solution framework. The red curve is unpreconditioned and the green curve shows the performance of a diagonal block preconditioned approach. While the diagonal preconditioner is very simple and a rather poor approximation of the problem being solved (all the coupling terms are missing), it is still significantly better than no preconditioner at all. The blue curve shows a lower-triangular preconditioner, and the pink curve is a lower triangular preconditioner using two block Gauss-Seidel sweeps to provide an approximate inverse. Note that each preconditioner requires more effort to form and invert, but this extra effort pays off in fewer GMRES iterations needed to solve the linear system.

4 BENCHMARK RESULTS

Figures 2 and 3 shows the results of the coupled thermomechanics and oxygen diffusion equation system solved using the JFNK method. The results obtained are similar to both Newman (2009) and Ramirez (2006). Unlike those approaches, the results in Figure 2 explicitly include the cladding in the simulation geometry, and the gap between the pellet and cladding is meshed using gap elements. Figure 3 shows the

transient response of the system and the dynamical time step chosen to resolve the coupled multiphysics problem. The timestepping algorithm is a variation of that proposed by Pope et. al. (2007).

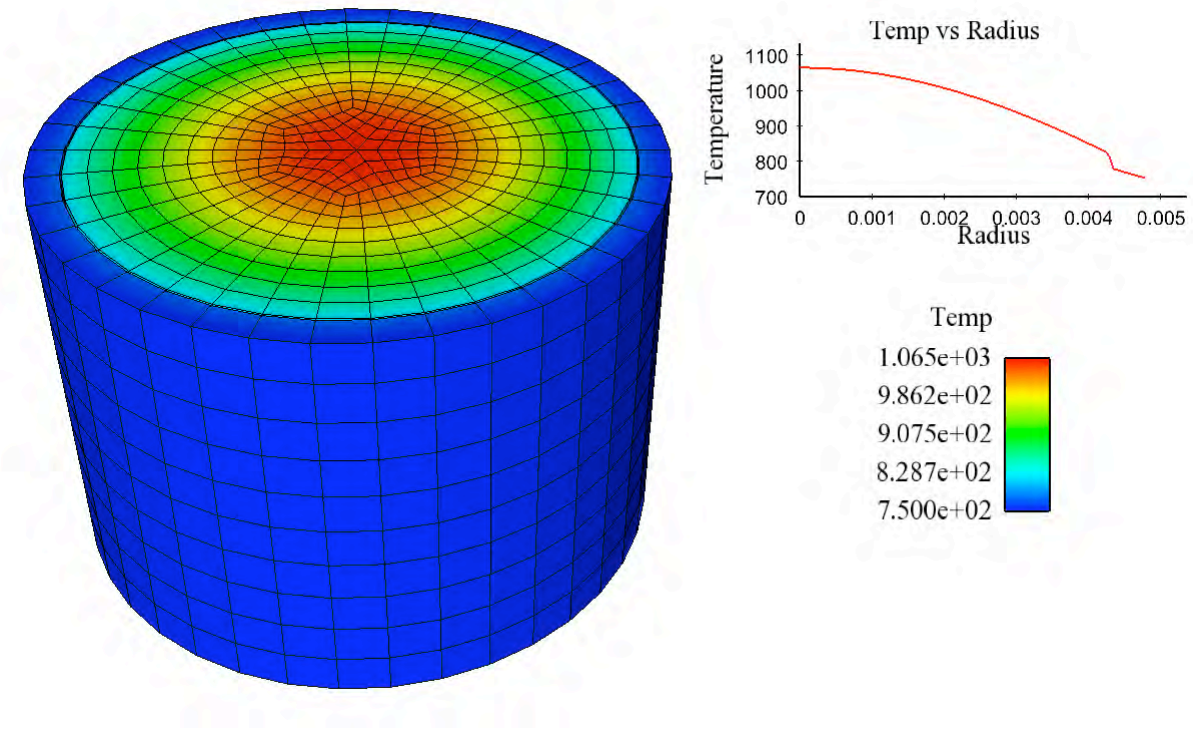

Figure 2. Steady state gap / cladding system simulation, using the approach advanced by Newman (2009) and the correlations presented therein. The temperature profile matches the results shown in the paper and also those presented in Ramirez (2006).

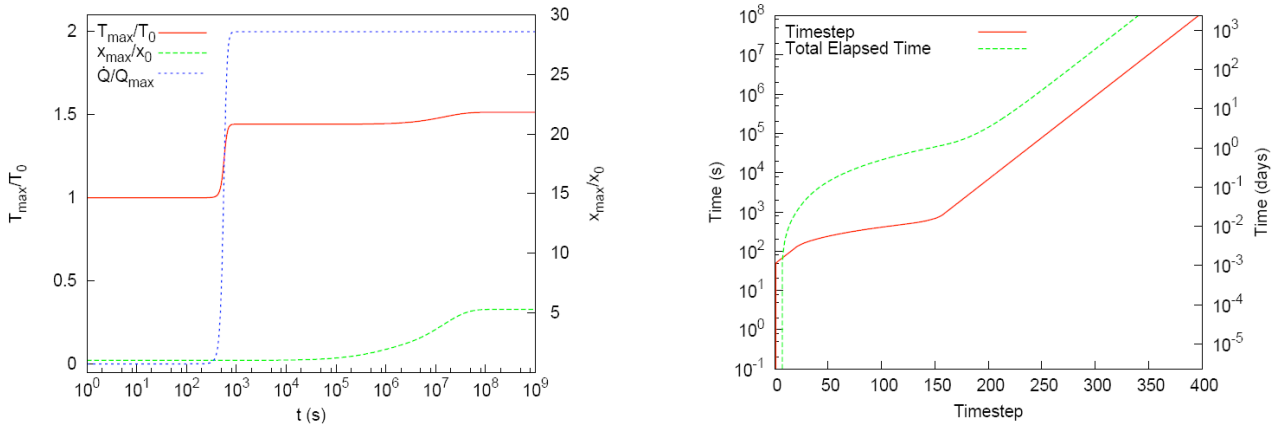

(a) Transient response **(b)** Timestep history

Figure 3. Results of transient calculation. Figure (a) shows transient response for reactor start up from ambient conditions for comparison with Figure 6 in Ramirez (2006) (and using $\dot{Q}(t)$ given in that paper). In these results, s_o = 0.01. Figure (b) shows the timestep history of the transient calculation.

5 PELLET / CLADDING COUPLED SIMULATION

The next set of calculations consider the displacement of the pellet as it undergoes thermal expansion of the fuel, followed by additional expansion driven by fission product formation within the ceramic under irradiation. The pellet swells both radially and axially over time, and the gap width decreases over time

(decreasing the thermal resistance across the gap). In time, the pellet outer surface touches the inner surface of the cladding and begins to displace the cladding outward. Figure 4 shows a three dimensional mesh of a calculation at the point where the top ridge of the pellet is just touching the cladding. The boundary condition of zero axial displacement is applied at the bottom of the pellet and at the bottom of the cladding segment shown in the picture. Further, the meshes initially match between the pellet and cladding, axially. At the time that the pellet swells to contact the cladding, note that significant axial displacement of the top of the pellet has occurred relative to the cladding.

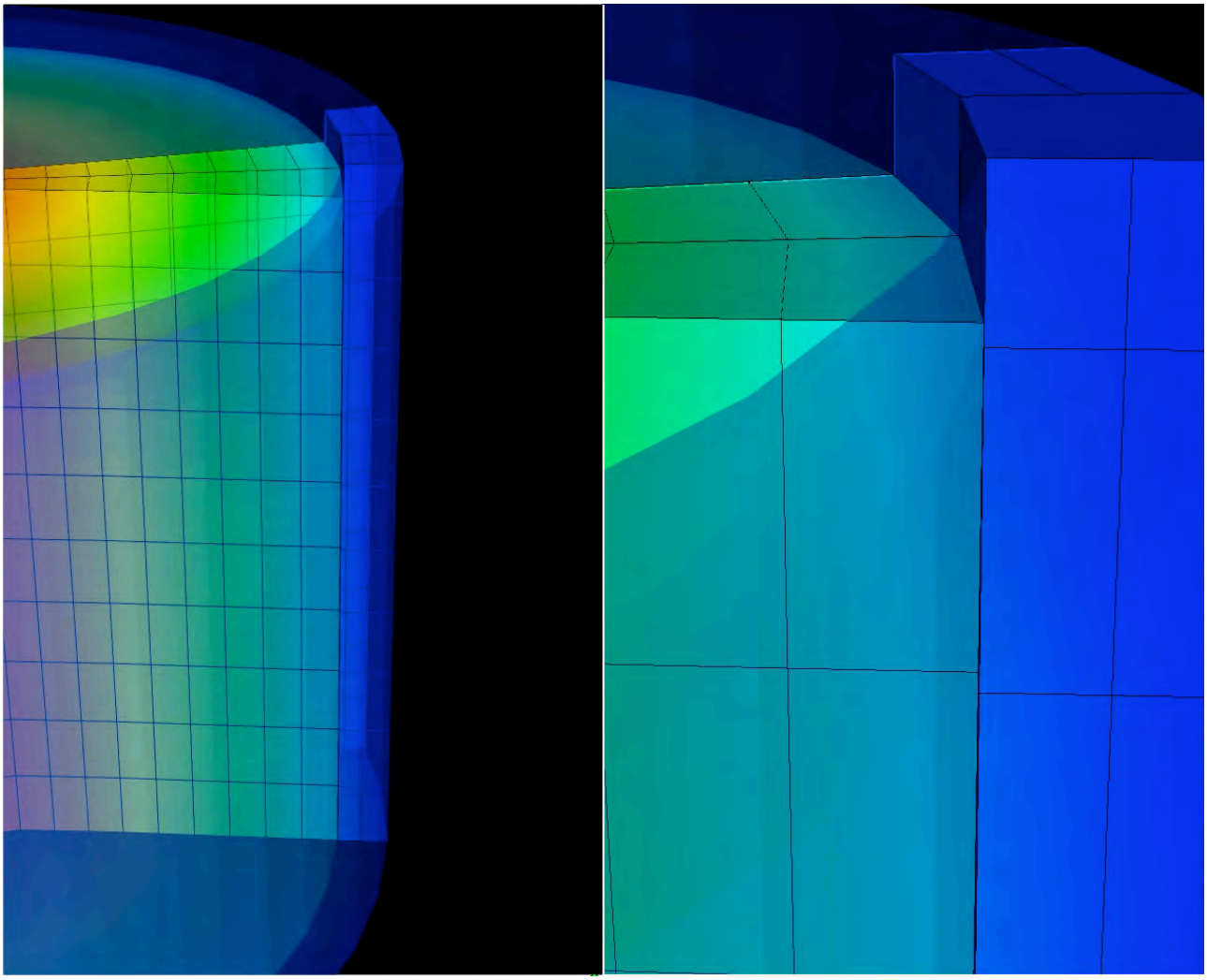

Figure 4. Representative calculation of a coupled thermomechanical calculation of a pellet / cladding system, at the point where the pellet is just beginning to touch the cladding. Left image shows a translucent view, with color indicating temperature. Right view is a closeup view of the top rim of the pellet.

Figure 5 shows the simulation much further out in time, where the pellet has expanded into the cladding and created significant displacement (and stresses) in the cladding. In this diagram, displacement is exaggerated, according to the caption, to show how the geometry of the pellet and cladding changes over time. Note the “bambooing” of the cladding caused by the deformed cylindrical pellet profile. Also, the geometry of this calculation is simplified; oxide fuel pellets are usually dished to limit axial expansion and chamfered to reduce the swelling at the top of the pellet. These details will be added in future work.

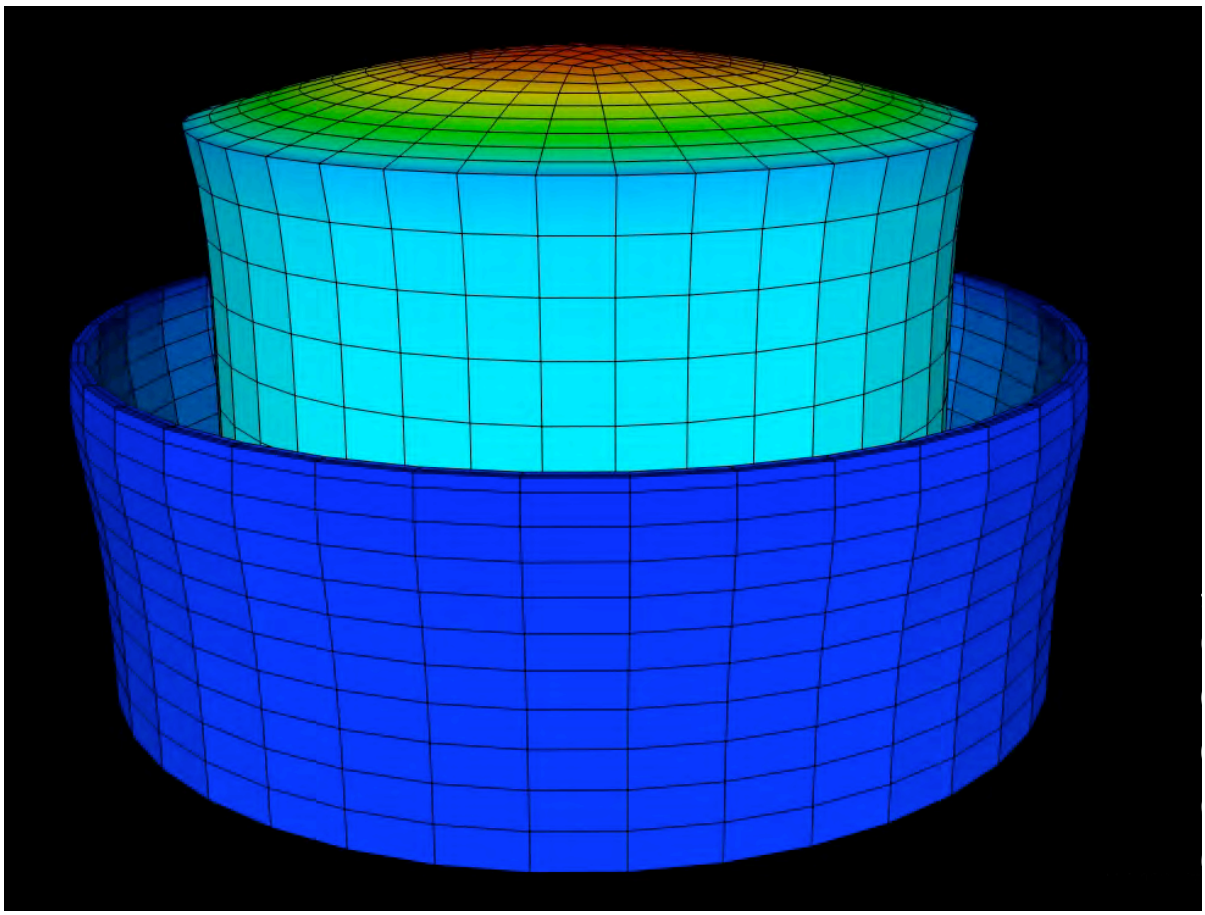

Figure 5. Exaggerated displacement of the pellet and cladding shown in Figure 4. The displacement of the cladding is exaggerated by a factor of 1000 to show the "bambooing" of the cladding caused by the contact of the pellet. Pellet deformation is exaggerated by 100 and offset to show the outside profile of the pellet. Color indicates relative temperature.

6 MULTISCALE MULTIPHYSICS SIMULATION

One fundamental limitation of the preceding finite element based simulation capability is the use of correlations and experimentally-derived data to close the partial differential equation models used in BISON. While light water reactor fuel data is quite plentiful and routinely used for this purpose, data applicable to extended burnup situations is harder to come by. Further, to design new fuels and new fuel geometry, existing data may not be fully appropriate. It would be advantageous to develop the capability to link "engineering scale" fuel performance codes like BISON to mesoscale (and below) simulation tools capable of calculating the fundamental behaviour of the fuel and cladding at these smaller scales to close the engineering scale finite element problem. Secondly, it is not generally practical to perform a pellet, or multiple pellet, calculation using a mesoscale code alone. The amount of computing power necessary to do so is not generally available.

In the previous development, it was argued that proper treatment of the coupling between the equations and correlations is beneficial. One would expect the engineering scale solution to be strongly dependent on the results of the mesoscale calculation, as it is on the correlations that describe the material behaviour. Further, one would expect that the engineering scale solution would provide the boundary conditions for multiple mesoscale simulations, performed at strategic locations within the engineering scale geometry; perhaps under conditions of temperature beyond where there is good data from correlations. Figure 6 is a schematic of this proposed engineering scale / mesoscale linkage; defined as both a multiscale and as a multiphysics problem. Consider an example of calculating heat conductivity of UO_2 within a mesoscale calculation and using this value in an engineering scale finite element calculation.

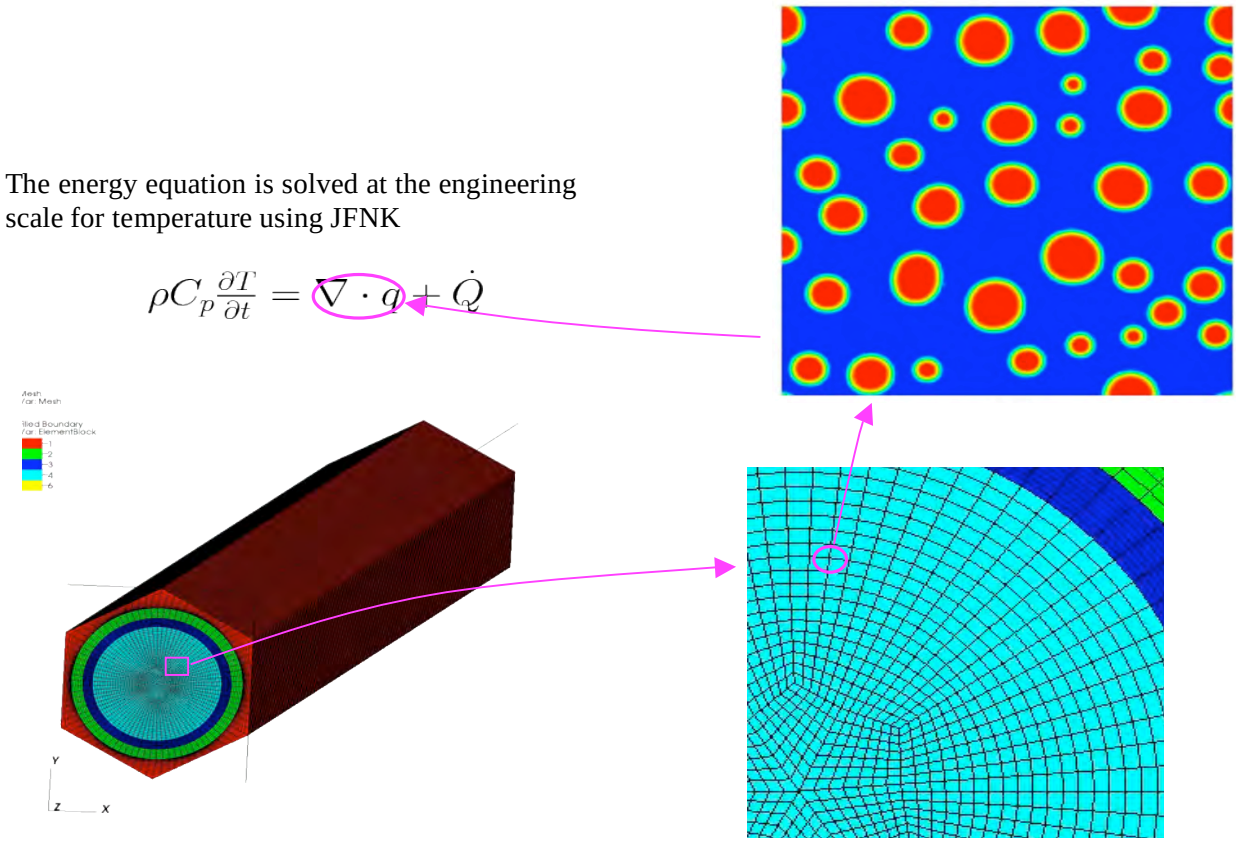

Figure 6. Multiscale multiphysics coupling schematic for calculation of thermal conductivity using a mesoscale phase-field simulation. The phase-field calculation uses the approach advanced by Rokkam et. al. (2008).

First, an engineering scale calculation is performed using an assumed thermal conductivity *k* or a value from the best available correlation. The strategic locations within the engineering scale are then chosen, for example those Gauss points with the highest temperature. At each of these Gauss points, a mesoscale calculation is initiated that is passed the temperature at the location. Many phase field calculations, perhaps similar to that proposed by Rokkam (2008), are performed in parallel; one per chosen Gauss point. A thermal conductivity is calculated at the mesoscale, and then upscaled to the engineering scale calculation. This new thermal conductivity is employed for an updated engineering scale solution. This process must be repeated until convergence is achieved given this explicit example. However, note that this example just described a coupled multiphysics problem; it can also be solved in a fully coupled manner simultaneously with the engineering scale problem using JFNK.

Figure 7 shows the results of a fully-coupled phase field / engineering scale solution solved with JFNK within BISON. The mesoscale results are shown at a single Gauss point; note the evolution of the voids within the phase field result over time. This coupled JFNK solution has proven quite effective and is quite scalable on a parallel computer as described. Left for future work is a more sophisticated strategy for determining which Gauss points should host the mesoscale solution(s).

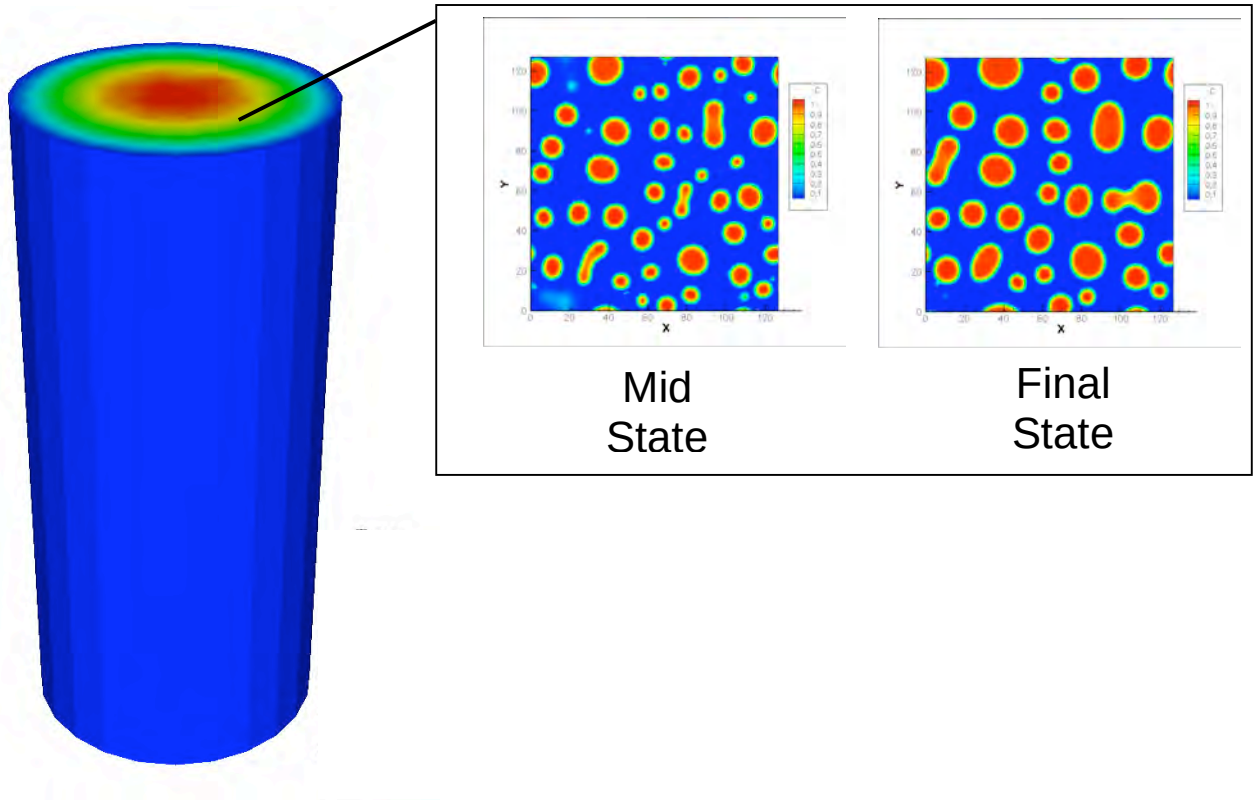

Figure 7. Representative thermal calculation showing changes in mesoscale void volume over time at a particular location (Gauss point).

The next advance for the BISON fuel performance capability is to directly solve the phase field problem in a three dimensional calculation without calling an auxiliary code to calculate the thermal conductivity. To begin to explore this requirement, the Cahn-Hilliard 4th-order equation

$$\frac{\partial c}{\partial t} = \nabla \cdot M_c \nabla (f_0'(c) - \epsilon_c^2 \Delta c)$$

was solved using JFNK and using $C^{(1)}$ continuous finite elements to allow its direct solution. The results of the Cahn-Hilliard solution are shown in Figure 8, where a two dimensional result is the left figure and a three dimensional solution is shown to the right. These results employed a mobility

$$M_c = I,$$

an epsilon

$$\epsilon_c = .01,$$

and a mathematical free-energy function derivative

$$f_0'(c) = c^3 - c.$$

One might visualize this solution as a water surface on which oil was sprayed. Over time the oil drops tend to gather, separated by ever larger volumes of water. The colors correspond to the spatial concentration of the two components at a particular time. These images are a snapshot at a given time of a transient movie.

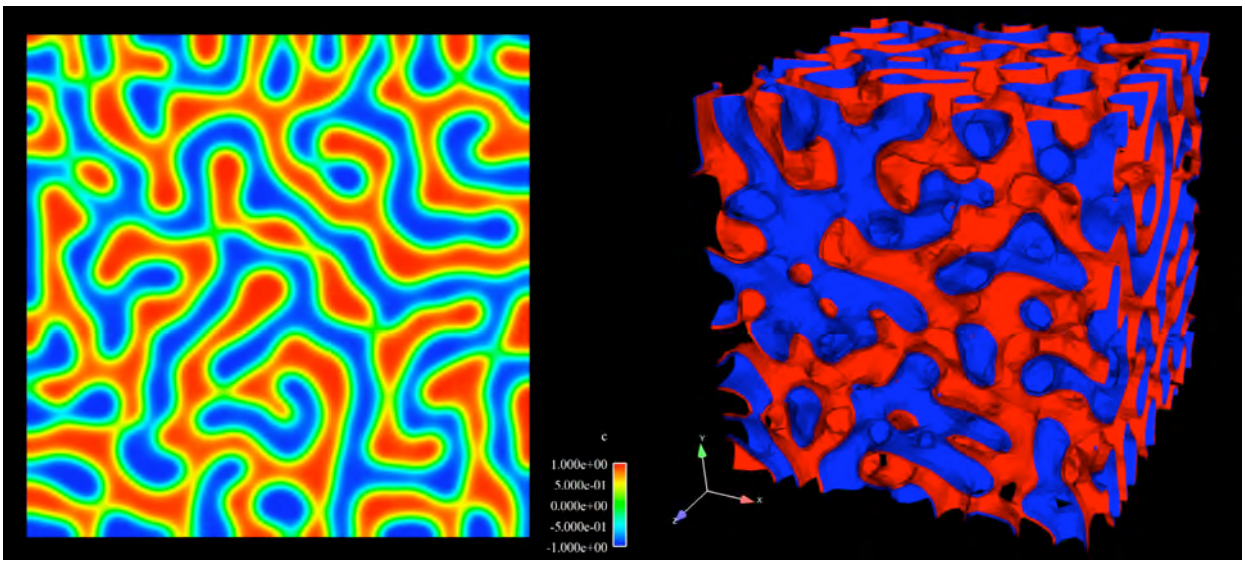

Figure 8. Spinodal decomposition: two and three dimensional solutions of the Cahn-Hilliard equation system.

7 CONCLUSION

This work explored the use of a software platform, BISON, for the calculation of a fully-coupled equation system describing a mock fuel performance problem. The equations of thermomechanics and oxygen diffusion were solved using the JFNK method and the results were compared to literature. The JFNK solution method showed itself to be very capable for this application.

Next, explicit cladding geometry was added to the above model and several representative calculations were performed. Lastly, a set of calculations were conducted to begin to study issues with multiscale multiphysics coupling using JFNK, by coupling a phase field mesoscale solution to the above engineering scale fuel performance calculation. The results, while currently limited in scope, were very encouraging.

Acknowledgements. *Work supported through the INL Laboratory Directed Research & Development (LDRD) Program under DOE Idaho Operations Office Contract DE-AC07-05ID14517 (INL/CON-09-15900).*

REFERENCES

Hohorst, J., 1990 SCDAP/RELAP5/MOD2 Code Manual, Volume 4: MATPRO–A Library of Materials Properties for Light-Water-Reactor Accident Analysis, Tech. rep., NUREG/CR-5273, EGG-2555

Knoll, D.A., and Keyes, D.E., 2004 Jacobian-Free Newton-Krylov Methods: a Survey of Approaches and Applications, J. Comput. Phys., Vol.193:2, P.357–397

Newman, C., Hansen, G., and Gaston, D., 2009 Three Dimensional Coupled Simulation of Thermomechanics, Heat, and Oxygen Diffusion in UO_2 Nuclear Fuel Rods, J. Nuclear Materials, in press

Pope, M.A., and Mousseau, V.A., 2007 Accuracy and Efficiency of a Coupled Neutronics and Thermal Hydraulics Model, in The 12th International Topical Meeting on Nuclear Reactor Thermal Hydraulics (NURETH-12), Sheraton Station Square, Pittsburgh, Pennsylvania, U.S.A., Log Number: 239

Ramirez, J., Stan, M., and Cristea, P., 2006 Simulations of heat and oxygen diffusion in UO_2 nuclear fuel rods, J. Nucl. Materials, Vol. 359:3, P.174–184

Rokkam, S.K., Millett, P.C., Wolf, D., and El-Azab, A., 2008 Phase Field Simulation of Void Growth in Irradiated Materials, Proceedings of the Fourth International Conference on Multiscale Materials Modeling, Symposium 4-Multiscale modeling of microstructure evolution in materials, P. 405-408

Saad, Y., 1995 Iterative Methods for Sparse Linear Systems, The PWS Series in Computer Science, PWS Publishing Company, Boston, MA